Environmental Science
Processes & Impacts

Accepted Manuscript

ROYAL SOCIETY
OF **CHEMISTRY**

rsc.li/process-impacts

Table of contents entry

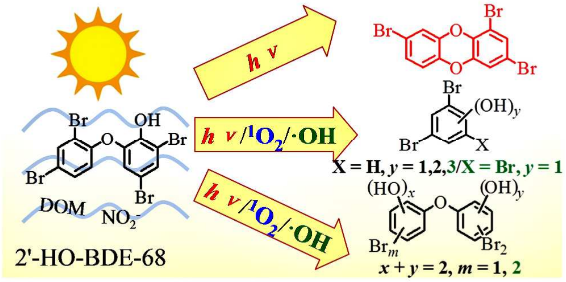

Photoproducts of 2'-HO-BDE-68 from different pathways were distinct. 1,3,8-tribromodibenzo-*p*-dioxin was produced from direct photolysis. Formation of di-HO-PBDEs was experimentally confirmed.

Environmental impact

Hydroxylated polyhalodiphenyl ethers (HO-PXDEs) are emerging aquatic pollutants, which can photogenerate polyhalodibenzo-*p*-dioxins (PXDDs) and other toxic products. In this study, the photochemical pathways (including direct photolysis and $^1O_2$/·OH oxidation) responsible for these photoproducts were clarified, taking 2'-HO-BDE-68 as a case. 1,3,8-tribromodibenzo-*p*-dioxin was found to be produced only from direct photolysis. The formation of di-HO-PBDEs was firstly experimentally confirmed and 2',5'-HO-2,3',4-tribromodiphenyl ether was proposed as a main direct photohydrolysis product. Yields of the products, which are irrespective of reaction time and can be employed for comparing the ability of different HO-PXDEs to photogenerate a given product, were also reported. This study implies that for accurate risk assessment of HO-PXDEs, the photoproducts from different photoreaction pathways should be considered.

Distinct photoproducts of hydroxylated polybromodiphenyl ethers from different photodegradation pathways: A case of 2'-HO-BDE-68[†]

Qing Xie, Jingwen Chen[*], Hongxia Zhao, Xingbao Wang, and Hong-Bin Xie

Key Laboratory of Industrial Ecology and Environmental Engineering (Ministry of Education), School of Environmental Science and Technology, Dalian University of Technology, Dalian 116024, China

Abstract

Hydroxylated polyhalodiphenyl ethers (HO-PXDEs) are emerging aquatic pollutants. Previous studies have shown that HO-PXDEs can photogenerate dioxins and phenolic compounds. However, it is unclear which photochemical pathways are responsible for the photoproducts. This study investigated the direct photolysis and photooxidation initiated by $^1O_2$ and ·OH that can be formed by photosensitization, taking 2'-HO-2,3',4,5'-tetrabromodiphenyl ether (2'-HO-BDE-68) as a case. The results show that 1,3,8-tribromodibenzo-*p*-dioxin can only be produced in the direct photolysis. By mass spectrum analysis, four dihydroxylated polybromodiphenyl ethers generated from both the direct and the indirect photodegradation were confirmed. Among them, di-HO-tribromodiphenyl ether (di-HO-TBDE) was a main product generated from the direct photohydrolysis. Most probably, the di-HO-TBDE is 2',5'-HO-2,3',4-tribromodiphenyl ether, as was suggested by density functional theory calculation. Ether bond cleavage is a dominant pathway for the direct photolysis and the photooxidation reactions, leading to 2,4-dibromophenol as the dominant product. Yields of the products, which are irrespective of reaction time and can be employed for comparing the ability of different HO-PXDEs to

---

[†] Electronic Supplementary Information (ESI) available: details of the total ion chromatograms and mass spectra of the identified products, the product yields, and the formation and degradation rate constants.

[*] Correspondence to: Jingwen Chen, e-mail: jwchen@dlut.edu.cn; Phone: +86-411-8470 6269

photogenerate a given product, were reported. This study indicates that for accurate ecological risk assessment of HO-PXDEs, their different photodegradation pathways that may lead to different photoproducts should be considered.

Keywords: hydroxylated polybromodiphenyl ether, photodegradation, photoproduct, halogenated dibenzo-*p*-dioxin

Introduction

Hydroxylated polyhalodiphenyl ethers (HO-PXDEs), such as the widely used antimicrobial triclosan and hydroxylated polybromodiphenyl ethers (HO-PBDEs), are frequently detected in various aqueous environments with the levels up to pg/L ~ ng/L in surface water, and μg/g in aquatic biotas.[1-3] They have attracted increasing concerns due to not only their frequent detection potential extensive sources,[2-6] and toxicity such as endocrine disrupting effects,[7,8] but also the risk caused by environmental transformation of HO-PXDEs. Photochemical reaction has been proved to be an important transformation pathway of HO-PXDEs in waters,[9-18] and halogenated dibenzo-*p*-dioxins (PXDDs) have been reported as the photoproducts of dozens of HO-PXDEs (e.g., triclosan and its chlorinated derivatives; 6-HO-BDE-47, 85, 90 and 99; 6'-HO-BDE-100 and 118; 2'-HO-BDE-68, 2-HO-BDE-123).[10-17]

The HO-PXDEs containing an ortho-hydroxyl to the ether linkage and an ortho-halogen atom on another ring were proposed to photogenerate PXDDs in waters. [13,16,17] The PXDD yields range from 0.1% to 12%, and depend on the halogenation patterns, ionization states of HO-PXDEs, and water constituents.[10,12,13,15-17] By density functional theory (DFT) calculation, Cao et al. also suggested that PXDDs can be formed via the gaseous reaction of HO-PXDEs with ·OH.[19]

Nevertheless, although it is known that organic pollutants can undergo both direct photolysis and indirect photolysis initiated by reactive oxygen species (e.g. ·OH, $^1O_2$) that are generated through light absorption of photosensitizers (e.g. dissolved organic matter, NO_3^-/NO_2^-, etc.),[20-22] it is still unknown whether all these aqueous photochemical processes are responsible for the formation of PXDDs from HO-PXDEs, and which process is dominant. The knowledge on the photoproducts from different photochemical pathways is of great importance to predict the PXDD yield and to assess the risk of HO-PXDEs in different sunlit waters.

In addition to PXDDs, other photoproducts of HO-PXDEs have also been detected.[10,11,16,23-26] Triclosan and its chlorinated derivatives (HO-PCDEs) were found to photogenerate polychlorodibenzo-*p*-dioxins (PCDDs), dechlorinated products, chlorophenols, triclosan isomers, and triclosan dimmers, under different conditions.[10,11,23-26] Recently, Erickson et al. investigated the direct photolysis products of three pentabrominated HO-PBDEs (6-HO-BDE-99, 6'-HO-BDE-100 and 6'-HO-BDE-118), and identified bromophenols, trace amounts of debrominated products, tetrabromo-HO-dibenzofurans, in addition to polybromodibenzo-*p*-dioxins (PBDDs).[16] The mass spectrum employed in these studies also identified products that were supposed to be dihydroxylated PCDEs/PBDEs (di-HO-PCDEs/di-HO-PBDEs).[11,16,23] Lai et al. proved that di-HO-PBDEs with two -OH at para- or ortho- positions are more toxic than HO-PBDEs due to their high reactivity with DNA.[27] Thus, further studies are necessary to elucidate the non-PXDD photoproducts generated from the different photolysis pathways of HO-PXDEs.

This study aimed at elucidating the yield of PBDDs and other photoproducts generated from the different photolysis pathways, taking 2'-HO-2,3',4,5'-tetrabromodiphenyl ether (2'-HO-BDE-68) as an example. 2'-HO-BDE-68 was selected as it was detected in aquatic environments frequently.[2,3] Direct photolysis, $^1O_2$ and ·OH oxidation experiments were performed. In addition, density functional theory (DFT) calculation was performed to probe the main pathways for photogeneration of di-HO-PBDEs.

Materials and methods

Chemicals

2'-HO-BDE-68 was synthesized in-house following Marsh et al.[28] Its purity was >98% as determined by high pressure liquid chromatograph (HPLC). 1,3,8-tribromodibenzo-*p*-dioxin (1,3,8-TBDD, 98.7%), 2,4-dibromophenol (2,4-DBP) and 2,4,6-tribromophenol (2,4,6-TBP) were purchased from AccuStandard. Rose bengal was purchased from Alfa Aesar. H_2O_2 (30%), $Fe_2SO_4 \cdot 7H_2O$, and borate (analytical reagent) were from Tianjin Kermel Chemical Reagent Co. 1% trimethylchlorosilane (TMCS) in N,O-bis(trimethylsilyl)trifluoroacetamide (BSTFA) was purchased from Sigma-Aldrich. Diazomethane was supplied by Dalian Kaifei Chemical Reagent Co. All organic solvents were of HPLC grade and purchased from Tedia. Ultrapure water (18 MΩ) was obtained from an OKP ultrapure water system produced by Shanghai Lakecore Instrument Co.

Photochemical experiment

The direct photolysis and $^1O_2$ photooxidation experiments were performed with an XPA-1 merry-go-round photochemical reactor (Xujiang Electromechanical Plant, China). In the direct photolysis experiment, a water-refrigerated 500 W high-pressure mercury lamp surrounded by 290 nm cutoff filters was employed to simulate the sunlight irradiation. The main irradiation wavelengths in the ranges of UV-A and UV-B include 297, 302, 313, 334, 365 and 366 nm.[18] For the $^1O_2$ photooxidation experiments, a 300 W high-pressure mercury lamp with 380 nm cutoff filters were used as the light source, and 6 μM rose bengal was used as the $^1O_2$ photosensitizer. The 380 nm cutoff filters only allow the light with the wavelengths of $\lambda > 380$ nm to be emitted. Thus, 2'-HO-BDE-68 has no photoabsorption under this irradiation condition and cannot undergo direct photolysis.[18] For the ·OH oxidation experiment, the conventional Fe^{2+}/H_2O_2 Fenton system was adopted with Fe^{2+} being sequentially added into the 2'-HO-BDE-68 solution containing 1.0 mM H_2O_2.[29] The 2'-HO-BDE-68 solution (4.0 μmol/L) used in the experiment was prepared with acetonitrile (0.5%, v/v) as cosolvent, and was adjusted to pH = 3 with sulfuric acid and pH = 10 with borate buffer (0.05 M). Periodically throughout the irradiation, one quartz tube containing 30 mL irradiated solution was withdrawn for product analysis.

Product analysis

In order to increase the abstraction efficiency of phenolic compound, each sample was acidified with HCl to pH<3, and then extracted with hexane and dichloromethane mixture (1:1) for 3 times. The organic phase was collected, dehydrated, and condensed to 1 mL in hexane. Then the concentrate was divided into two aliquots. For one aliquot (0.5 mL), 5 drops of methanol was added, and then diazomethane was added for derivatization (12 h, room temperature). For the other aliquot (0.5 mL), 5 drops of tetrahydrofuran was added, followed by addition of the trimethylsilylation reagent BSTFA+TMCS for derivatization (4 h, 60 ºC). The derivatized samples were evaporated to dryness by a gentle N_2 stream and redissolved with 0.5 mL hexane.

The final samples were analyzed with an Agilent 6890GC/5975MS. For details, see Text 1 of the Electronic Supplementary Information (ESI). Both electron-impact ionization (EI) source and negative chemical ionization (NCI, CH_4 as reaction gas) source were operated in the scan mode to identify the potential products. The structures of brominated dioxins were further confirmed by the authentic standards. Selected ion monitoring of $m/z = 79$ and 81 with the NCI source was adopted for quantification of the brominated compounds.

The product yield (Y) is defined as the ratio between the formation rate constant of a given product (k_{p}) and the degradation rate constant of 2'-HO-BDE-68 (k_{deg}).[16] The first-order formation and degradation rate constants (k_{p} and $k_{\mathrm{-p}}$) of each product were obtained by fitting the following kinetic equation,

$$[\mathrm{P}] = k_{\mathrm{p}} c_0 (\mathrm{e}^{-k_{\mathrm{deg}} \cdot t} - \mathrm{e}^{-k_{-\mathrm{p}} \cdot t})/(k_{-\mathrm{p}} - k_{\mathrm{deg}}) \quad (1)$$

where [P] refers to product concentration, c_0 is the initial concentration of 2'-HO-BDE-68. Thus, the definition of Y in this study encodes the information on both the product formation and the product degradation.

DFT calculation

Gaussian 09 program suite[30] was employed for the calculation. The MPWB1K functional[31] was adopted, as it has been proved with excellent performance in the prediction of thermochemical dynamics, and has been employed to successfully explore the formation of PXDDs. [32-34] The geometry optimization and harmonic frequency calculation of the reactants, products, and transition states (TS) were performed at the MPWB1K/6-31+G(d,p) level. The connection of the TS between designated pre-reactive complex and product complex was confirmed by the intrinsic reaction coordinate calculation.[35] Single point energy calculations were performed at MPWB1K/6-311+G(3df,2p) level based on the optimized geometries at the MPWB1K/6-31+G(d,p) level. Zero-point energy and thermal energy correction at MPWB1K/6-31+G(d,p) level were used to correct single point energy to obtain the final potential energies and thermodynamic energies such as Gibbs free energy and enthalpy.

The solvent effects of water were considered by the integral equation formalism polarized continuum model (IEFPCM) in the self-consistent-reaction-field (SCRF) method.[36] Charge (q) and electronic spin density (ρ) were calculated by the natural bond orbital (NBO) scheme.[37] The lowest excited triplet state (T_1) of 2'-HO-BDE-68 was designed as the reactant, as T_1 has longer life-time than the excited singlet state, and most photochemical reactions occur at T_1.[38-40]

Results and discussion

Photoproducts of direct photolysis

The pK_a for 2'-HO-BDE-68 is 6.63 ± 0.48.[18] Thus, 2'-HO-BDE-68 exists in neutral and anionic forms under the conditions of pH = 3 and 10, respectively. We identified four photoproducts from the direct photolysis under the two pH conditions: 2,4-dibromophenol (2,4-DBP), dihydroxylated dibromobenzene (di-HO-DBB), 1,3,8-tribromodibenzo-*p*-dioxin (1,3,8-TBDD) and dihydroxylated tribromodiphenyl ether (di-HO-TBDE). 2,4-DBP and 1,3,8-TBDD were confirmed and quantified with the authentic standards. For di-HO-DBB and di-HO-TBDE, the number of -OH groups was confirmed with the *m/z* differences between the samples derivatized by diazomethane and BSTFA+TMCS, and the number of Br atoms was confirmed by the isotope pattern of Br (Fig. 1). The total ion chromatograms and mass spectra for these products are shown in Fig. S1 and Fig. S2. The substitution patterns of -Br and -OH were not determined, due to the lack of authentic standards. As far as we know, this is the first experimental confirmation on the production of di-HO-PBDEs and di-HO-DBB.

The evolution of the four photoproducts and their kinetic profiles fitted with eq. (1) are shown in Fig. 2. The total yields of the identified products are (41 ± 14)% and (63 ± 22)% at the pH = 3 and pH = 10 conditions, respectively. The fitted k_p, k_{-p} and the calculated product yields are listed in Table S1. As no authentic standards for di-HO-DBB and di-HO-TBDE are available, they were quantified by the response factors of 2,4-DBP and 1,3,8-TBDD as they have the same bromination degrees with the corresponding two di-hydroxylated compounds. k_p and k_{-p} for the products are higher at pH = 10 than the corresponding values at pH = 3, especially for the phenolic products. The anionic species of halophenols (e.g. chlorophenols, tetrabromobisphenol A and related phenols) were also found to photodegrade faster than the corresponding neutral forms.[41,42] It is noteworthy that many previous studies reported an apparent product yield that was defined as concentration ratio between the product and the consumed parent compound. However, the apparent yield varies with reaction time, as the products can undergo further degradation. The product yield adopted in the current study is irrespective of reaction time, and can truly reflect the percent conversion of the parent and products.

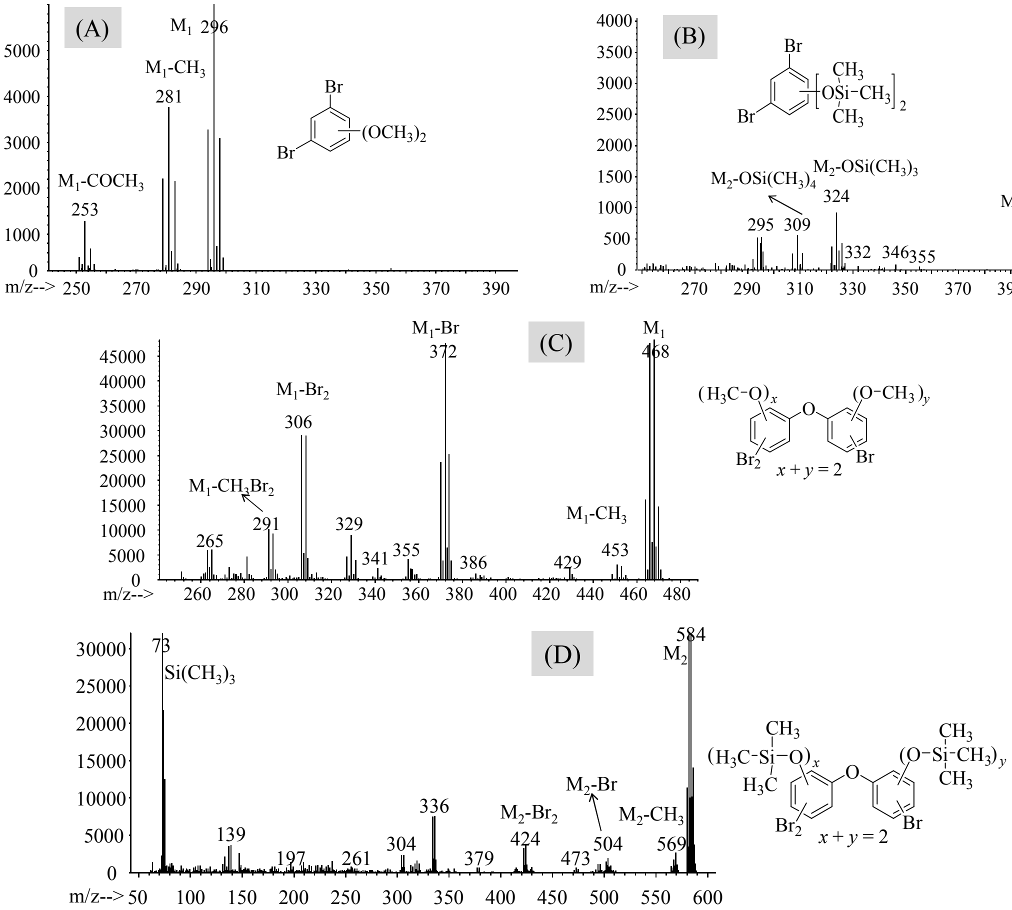

Fig. 1 Mass spectra (EI source) for diazomethane and BSTFA+TMCS derivatized di-HO-DBB (A, B) and di-HO-PBDEs (C, D) generated from direct hydrolysis of 2'-HO-BDE-68.

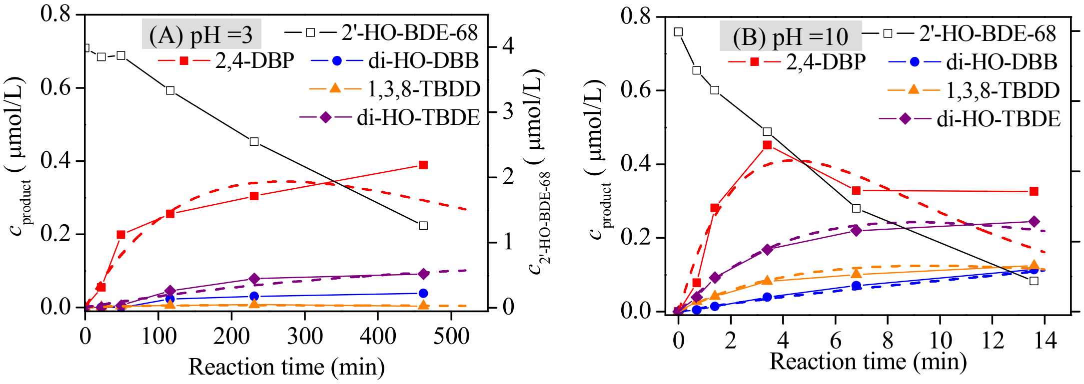

Fig. 2 Evolution of photoproducts from direct photolysis of 2'-HO-BDE-68, with the dash lines fitted by eq. (1).

The 1,3,8-TBDD yield in the basic solution [(5.9 ± 1.1)%] is much higher than that in the acidic solution [(0.86 ± 0.20)%]. Previous studies seldom reported the dioxin yields for the neutral forms of HO-PXDEs. Here, we found that dioxin can also be generated via direct photolysis of neutral 2'-HO-BDE-68, albeit the yield is much lower than that of the anionic form. Arnoldsson et al.[15] investigated photogeneration of PBDDs from HO-PBDEs dissolved in artificial coast waters, and their results indicated that apparent yields of PBDDs decreased with reaction time. Therefore, when presenting the yield of PXDDs, the concurrent photodegradation should not be neglected. In the current study, the yield (Y) of 1,3,8-TBDD was calculated by the ratio between the formation rate constant (k_p) and the degradation rate constant of 2'-HO-BDE-68 (k_{deg}), and the degradation rate of 1,3,8-TBDD has been considered with eq. (1) when calculating k_p. As far as we know, this is the first report on the yields of PXDDs with the consideration of their concurrent photodegradation. The yield adopted in the current study is an important indicator for comparing the ability of different HO-PXDEs to photogenerate PXDDs.

As can be seen from Fig. 2, 2,4-DBP is a main product for both the neutral [$Y = (35 \pm 13)\%$] and the anionic form of 2'-HO-BDE-68 [$Y = (43 \pm 18)\%$], confirming that ether bond cleavage is an important direct photolysis pathway.[18] We found when more than 60% of 2'-HO-BDE-68 was degraded under the two pH conditions, the detected concentrations of 2,4-DBP were higher than the fitted levels, suggesting that the degradation of other products (e.g., di-HO-TBDE) may also generate 2,4-DBP.

The yield of di-HO-TBDE in the basic solutions [(12 ± 2)%] is also higher than that in the acidic solutions [(3.4 ± 2.1)%]. Photohydrolysis of one C-Br bond of 2'-HO-BDE-68 can be the formation pathway of di-HO-TBDE.[42,43] For triclosan, products from photohydrolysis of C-Cl bonds have also been observed.[11] By the DFT calculation, we further evaluated the thermodynamics of photohydrolysis for the different C-Br bonds.

DFT insights into the photohydrolysis producing di-HO-TBDE

Eight possible photohydrolysis pathways corresponding to the 4 reaction sites (C_2, C_4, $C_{3'}$, and $C_{5'}$, shown in Table 1) and each site with H_2O and OH^- as attacking nucleophiles were calculated for both the neutral and anionic 2'-HO-BDE-68 at triplet excited state (T_1). For each pathway, one transient state was located that connects both the reactant complex and the product complex. The computed Gibbs free energy changes (ΔG), enthalpy changes (ΔH) and activation energies ($\Delta E^{\ddagger}$) for these pathways are listed in Table 1. For all the pathways with OH^- as the nucleophile, the ΔG and ΔH values are negative and the $\Delta E^{\ddagger}$ values are much lower than those pathways with H_2O as the nucleophile. These results indicate that the OH^- catalyzed photohydrolysis pathways are thermodynamically spontaneous and exothermic, and the hydrolysis of 2'-HO-BDE-68 occurs favorably in solutions with high pH values. The calculation results have been proved by the experimental observation that the yield of di-HO-TBDE in the basic solution was higher than that in the acidic solution. Furthermore, we found that the $\Delta E^{\ddagger}$ values for the pathways at site $C_{5'}$ are the lowest for both neutral and anionic 2'-HO-BDE-68 attacking by H_2O/OH^-, followed by the values corresponding with the $C_{3'}$ site, suggesting that the C-Br bonds at the phenolic ring tend to hydrolysis favorably. In addition, the $\Delta E^{\ddagger}$ values for the pathways at site $C_{5'}$ are much lower than those at the other sites, suggesting that 2',5'-dihydroxy-2,3',4-tribromodiphenyl ether is the most probable photohydrolysis product from the direct photolysis.

Fig. 3 shows the optimized structures of the pre-reaction complex (RC), transition state (TS) and product complex (PC) for OH^- catalyzed hydrolysis of the $C_{5'}$-Br bond of anionic 2'-HO-BDE-68 at T_1 state. Compared with the ground state, the $C_{5'}$-Br bond of RC has been evidently elongated from 1.88 Å to 2.70 Å upon photoexcitation. In the TS, the bond length was further elongated, and the charge of $Br_{5'}$ is -0.87, indicating that anionic 2'-HO-BDE-68 undergo heterogeneous cleavage of the $C_{5'}$-Br bond. The electronic spin density of $C_{5'}$ in the TS is 1.18, indicating a radical reaction process. For the PC, a leaving Br^- and a new $C_{5'}$-OH bond were formed.

Table 1 Computed Gibbs free energy changes (ΔG), enthalpy changes (ΔH) and activation eergies ($\Delta E^{\ddagger}$) for the dferent potohydrolysis pthways of nutral and aionic 2'-HO-BDE-68 at triplet excited state

Reaction site 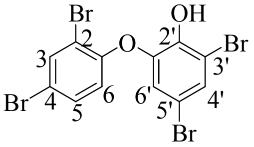	H_2O as nucleophile (kcal/mol)			OH^- as nucleophile (kcal/mol)		
	ΔG	ΔH	$\Delta E^{\ddagger}$	ΔG	ΔH	$\Delta E^{\ddagger}$
C_2-neutral molecule	-3.08	-2.63	59.4	-59.3	-60.2	10.1
C_2-anion	-1.73	-1.90	56.7	-58.0	-59.5	15.3
C_4-neutral molecule	-1.63	-2.08	52.3	-57.9	-59.7	16.2
C_4-anion	-1.56	-2.08	53.2	-57.8	-59.7	17.6
$C_{3'}$-neutral molecule	-2.40	-2.85	26.1	-58.7	-60.4	8.40
$C_{3'}$-anion	-2.50	-2.62	46.3	-58.8	-60.2	3.29
$C_{5'}$-neutral molecule	5.34	4.53	16.5	-50.9	-53.1	13.0
$C_{5'}$-anion	-1.34	-2.88	28.2	-57.6	-60.5	0.98

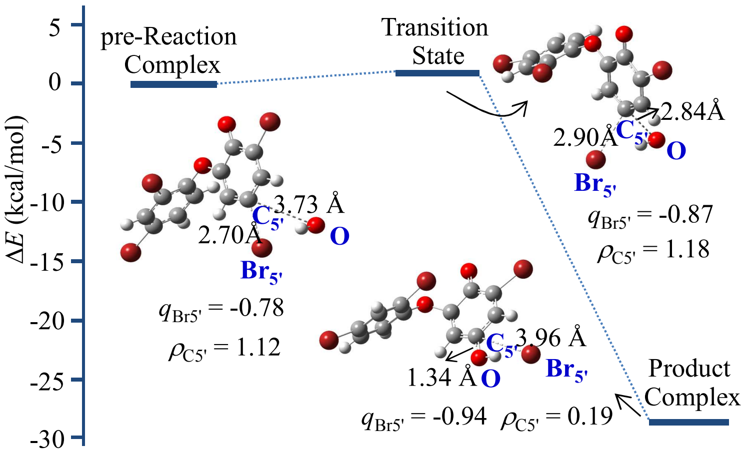

Fig. 3 Potential energy profile for OH^- catalyzed hydrolysis of $C_{5'}$-Br bond of anionic 2'-HO-BDE-68 at triplet excited state, with the optimized structures of the pre-reaction complex, transition state and product complex ($q_{Br5'}$ and $\rho_{C5'}$ represent the charge distributed in $Br_{5'}$ and electronic spin density distributed in $C_{5'}$).

Photoproducts of $^1O_2$ reaction

In most fresh and seawaters, 2'-HO-BDE-68 mainly presents in the anionic form (70.1% at pH = 7 and 97.3% at pH = 8.1). We also found that the reactivity of anionic 2'-HO-BDE-68 with $^1O_2$ was about 34 times higher than that of the neutral forms.[18] Thus, we analyzed the products from the reaction of anionic 2'-HO-BDE-68 with $^1O_2$. Four products were identified, including 2,4-DBP, di-HO-DBB, and di-HO-TBDEs with two different substitution patterns. One di-HO-TBDE was the same as that detected in the direct photolysis as was confirmed by a same GC retention time. The total ion chromatograms of these products are shown in Fig. S3. 1,3,8-TBDD was not detected in the $^1O_2$ oxidation reaction. The evolution of the photoproducts is shown in Fig. 4 and the fitted k_p and k_{-p} values are listed in Table S2. 2,4-DBP was a dominant product, for which the yield [(70 ± 25)%] is much higher than those in the direct photolysis. The good fit of the kinetic profile of eq. (1) implies that 2,4-DBP was mainly produced from the $^1O_2$ oxidation of 2'-HO-BDE-68. Latch et al. also found that

2,4-dichlorophenol is the main $^1O_2$ oxidation products of triclosan with the yield about 79%.[24] The total yield of di-HO-TBDEs is less than 0.4%, which is much lower than those in the direct photolysis.

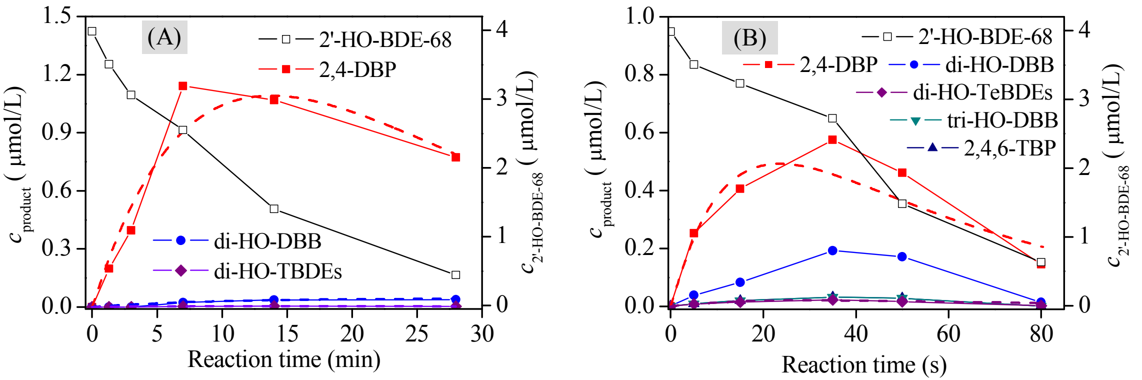

Fig. 4 Evolution of the identified products from the $^1O_2$ (A) and ·OH (B) oxidation of 2'-HO-BDE-68.

Products of ·OH reaction

As the Fenton reagent performed much better in acidic solutions than in neutral and basic solutions, the products from the reaction of 2'-HO-BDE-68 with ·OH at pH = 3 were analyzed. Six products were identified, including 2,4-DBP, di-HO-DBB, 2,4,6-tribromophenol (2,4,6-TBP), trihydroxydibromobenzene (tri-HO-DBB), and two dihydroxylated tetrabromodiphenyl ethers (di-HO-TeBDEs) with different GC retention times. PBDDs and di-HO-TBDEs were not detected. The total ion chromatogram and mass spectra for 2,4,6-TBP, tri-HO-DBB and di-HO-TeBDEs were shown in Fig. S4 and Fig. S5. The mass spectrum and GC retention time of 2,4,6-TBP were further confirmed with the authentic standard. Di-HO-TeBDEs were quantified with the response factor of 2'-HO-BDE-68.

The evolution of these products is shown in Fig. 4B, and the fitted k_{p} and $k_{\text{-p}}$ values are listed in Table S2. Similar to the $^1O_2$ initiated oxidation, 2,4-DBP is also a dominant product, for which the yield is (75 ± 15)%, and the yield of di-HO-TeBDEs [(2.4 ± 0.8)%] is very low. We found that the apparent yield of di-HO-DBB first increased and then decreased with the proceeding of the reaction (Table S3). As di-HO-DBB can be generated from the reaction of ·OH with both 2'-HO-BDE-68 and 2,4-DBP, the kinetic profile of di-HO-DBB cannot be fitted with eq. (1). Similarly, as 2,4,6-TBP and tri-HO-DBB are secondary products from the reaction of ·OH with 2'-HO-BDE-68, their kinetic profiles cannot be fitted with eq. (1) either. The production of 2,4,6-TBP implies that bromine radical may involve in the reaction. Nevertheless, the route for generating 2,4,6-TBP can't be infer yet.

Implications

We have totally identified 9 photoproducts from the direct photolysis of 2'-HO-BDE-68 as well as the oxidation of 2'-HO-BDE-68 by ·OH and $^1O_2$. In sunlit surface waters, the photoabsorption of dissolved organic matter and inorganic anions (e.g. NO_3^-, NO_2^-) can generate the reactive oxygen species (e.g. $^1O_2$, $O_2^{\cdot -}$, ·OH), and $O_2^{\cdot -}$ can be transformed into H_2O_2 and ·OH by dismutation. [20-22,44] Thus, the identified products represent those that can be formed in the direct and indirect photolysis of 2'-HO-BDE-68. Among the identified products, 2,4,6-TBP and tri-HO-DBB are newly identified, and four di-HO-PBDEs were firstly confirmed in this study.

Based on the products, we can summarize the photodegradation pathways of 2'-HO-BDE-68, as shown in Fig. 5. For the first time, the photodegradation pathways that are responsible for the main photoproducts have been clarified. Cleavage of the ether bond is the dominant pathway for the direct photolysis as well as the $^1O_2$ and ·OH reactions, leading to 2,4-DBP as the dominant product. Direct photohydrolysis is a main pathway for generating the di-HO-PBDEs, although di-HO-PBDEs were also detected in the $^1O_2$ and ·OH initiated reactions. An important finding of this study is that 1,3,8-TBDD can only be formed in the direct photolysis. The formed di-HO-PBDEs deserve special concerns as their high reactivity with DNA can result in chromosomal alternations.[27,45,46] Thus, for accurate ecological risk assessment of HO-PXDEs, their different photodegradation pathways that may lead to different photoproducts should be considered.

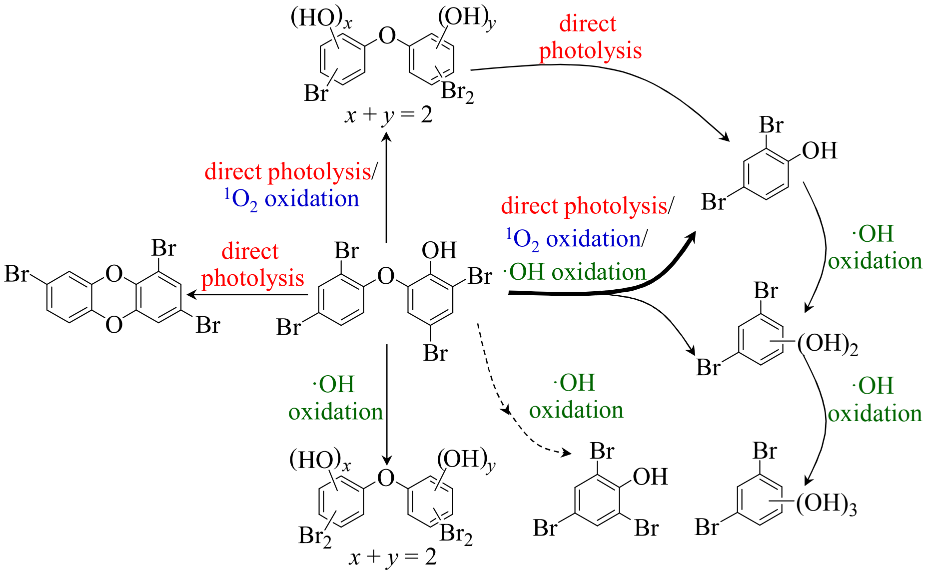

Fig. 5 Photodegradation pathways of 2'-HO-BDE-68 in direct photolysis, and $^1O_2$ and ·OH oxidation.

Acknowledgements

The study was supported by the National Basic Research Program (2013CB430403) and National Natural Science Foundation (21207013, 21277017, 21325729) of China.

Notes and references

1 H. Singer, S. Müller, C. Tixier, L. Pillonel, *Environ. Sci. Technol.,* 2002, **36**, 4998-5004.

2 A. Malmvärn, G. Marsh, L. Kautsky, M. Athanasiadou, Å. Bergman, L. Asplund, *Environ. Sci. Technol.,* 2005, **39**, 2990-2997.

3 D. Ueno, C. Darling, M. Alaee, G. Pacepavicius, C. Teixeira, L. Campbell, R.J. Letcher, Å. Bergman, G. Marsh, D. Muir, *Environ. Sci. Technol.,* 2008, **42**, 1657-1664.

4 K. Inaba, T. Doi, N. Isobe, T. Yamamoto, *Water Res.,* 2006, **40**, 2931-2937.

5 H.M. Stapleton, S.M. Kelly, R. Pei, R.J. Letcher, C. Gunsch, *Environ. Health Perspect.*, 2009, **117**, 197-202.

6 J. Zhou, J.W Chen, C.-H. Liang, Q. Xie, Y.-N. Wang, S.Y. Zhang, X.L. Qiao, X.H. Li, *Environ. Sci. Technol.*, 2011, **45**, 4839-4845.

7 R.F. Cantón, D.E. Scholten, G. Marsh, P.C. De Jong, M. Van den Berg, *Appl. Pharm.*, 2008, **227**, 68-75.

8 F. Li, Q. Xie, X.H. Li, N. Li, P. Chi, J.W. Chen, Z.J. Wang, C. Hao, *Environ. Health Persp.*, 2010, **118**, 602.

9 C. Tixier, H.P. Singer, S. Canonica, S.R. Müller, *Environ. Sci. Technol.*, 2002, **36**, 3482-3489.

10 D.E. Latch, J.L. Packer, W.A. Arnold, K. McNeill, *J. Photochem. Photobio. A*, 2003, **158**, 63-66.

11 P. Wong-Wah-Chung, S. Rafqah, G. Voyard, M. Sarakha, *J. Photochem. Photobio. A*, 2007, **191**, 201-208.

12 J.M. Buth, M. Grandbois, P.J. Vikesland, K. McNeill, W.A. Arnold, *Environ. Toxicol. Chem.*, 2009, **28**, 2555-2563.

13 P.O. Steen, M. Grandbois, K. McNeill, W.A. Arnold, *Environ. Sci. Technol.*, 2009, **43**, 4405-4411.

14 J.M. Buth, P.O. Steen, C. Sueper, D. Blumentritt, P.J. Vikesland, W.A. Arnold, K. McNeill, *Environ. Sci. Technol.*, 2010, **44**, 4545-4551.

15 K. Arnoldsson, P.L. Andersson, P. Haglund, *Environ. Sci. Technol.*, 2012, **46**, 7567-7574.

16 P.R. Erickson, M. Grandbois, W.A. Arnold, K. McNeill, *Environ. Sci. Technol.*, 2012, **46**, 8174-8180.

17 S. Kliegman, S.N. Eustis, W.A. Arnold, K. McNeill, *Environ. Sci. Technol.*, 2013, **47**,

6756-6763.

18 Q. Xie, J.W. Chen, H.X. Zhao, X.L. Qiao, X.Y. Cai, X.H. Li, *Chemosphere*, 2013, **90**, 188-194.

19 H.J. Cao, M.X. He, Y.H. Sun, D.D. Han, *J. Phys. Chem. A*, 2011, **115**, 13489-13497.

20 J. Mack, J.R. Bolton, *J. Photochem. Photobio. A*, 1999, **128**, 1-13.

21 P.R. Maddigapu, M. Minella, D. Vione, V. Maurino, C. Minero, *Environ. Sci. Technol.*, 2011, **45**, 209-214.

22 T. Zeng, W.A. Arnold, *Environ. Sci. Technol.*, 2012, **47**, 6735-6745.

23 I. Ferrer, M. Mezcua, M.J. Gómez, E.M. Thurman, A. Agüera, M.D. Hernando, A.R. Fernández-Alba, *Rapid Commun. Mass. Sp.*, 2004, **18**, 443-450.

24 D.E. Latch, J.L. Packer, B.L. Stender, J. VanOverbeke, W.A. Arnold, K. McNeill, *Environ. Toxicol. Chem.*, 2005, **24**, 517-525.

25 L. Sanchez-Prado, M. Llompart, M. Lores, C. García-Jares, J.M. Bayona, R. Cela, *Chemosphere*, 2006, **65**, 1338-1347.

26 Z.L. Chen, G.Q. Cao, Q.J. Song, *Environ. Chem. Lett.*, 2010, **8**, 33-37.

27 Y. Lai, M. Lu, X. Gao, H. Wu, Z. Cai, *Environ. Sci. Technol.*, 2011, **45**, 10720-10727.

28 G. Marsh, R. Stenutz, Å. Bergman, *Eur. J. Org. Chem.*, 2003, **2003**, 2566-2576.

29 E. Neyens and J. Baeyens, *J. Hazard. Mater.*, 2003, **98**, 33-50.

30 M.J. Frisch, G.W. Trucks, H.B. Schlegel, G.E. Scuseria, M.A. Robb, J.R. Cheeseman, G. Scalmani, V. Barone, B. Mennucci, G.A. Petersson, H. Nakatsuji, M. Caricato, X. Li, H.P. Hratchian, A.F. Izmaylov, J. Bloino, G. Zheng, J.L. Sonnenberg, M. Hada, M. Ehara, K. Toyota, R. Fukuda, J. Hasegawa, M. Ishida, T. Nakajima, Y. Honda, O. Kitao, H. Nakai, T.

Vreven, J.A. Montgomery, J.E. Peralta, F. Ogliaro, M. Bearpark, J.J. Heyd, E. Brothers, K.N. Kudin, V.N. Staroverov, R. Kobayashi, J. Normand, K. Raghavachari, A. Rendell, J.C. Burant, S.S. Iyengar, J. Tomasi, M. Cossi, N. Rega, J.M. Millam, M. Klene, J.E. Knox, J.B. Cross, V. Bakken, C. Adamo, J. Jaramillo, R. Gomperts, R.E. Stratmann, O. Yazyev, A.J. Austin, R. Cammi, C. Pomelli, J.W. Ochterski, R.L. Martin, K. Morokuma, V.G. Zakrzewski, G.A. Voth, P. Salvador, J.J. Dannenberg, S. Dapprich, A.D. Daniels, O. Farkas, J.B. Foresman, J.V. Ortiz, J. Cioslowski, D.J. Fox,. Gaussian 09, Revision A.02; Gaussian, Inc.: Wallingford, CT (2009).

31 Y. Zhao and D. G. Truhlar, *J. Phys. Chem. A*, 2004, **108**, 6908-6918.

32 F. Xu, W. Yu, Q. Zhou, R. Gao, X. Sun, Q. Zhang and W. Wang, *Environ. Sci. Technol.*, 2010, **45**, 643-650.

33 Q. Zhang, W. Yu, R. Zhang, Q. Zhou, R. Gao and W. Wang, *Environ. Sci. Technol.*, 2010, **44**, 3395-3403.

34 H. Cao, M. He, D. Han, J. Li, M. Li, W. Wang and S. Yao, *Environ. Sci. Technol.*, 2013, **47**, 8238-8247.

35 K. Fukui, *Accounts. Chem. Res.*, 1981, **14**, 363-368.

36 J. Tomasi, B. Mennucci and R. Cammi, *Chem. Rev.*, 2005, **105**, 2999-3094.

37 E.D. Glendening, A.E. Reed, J.E. Carpenter, F. Weinhold, NBO version 3.1, as implemented in Gaussian 03, revision, D. 01, Gaussian, Inc., Wallingford, CT (2004).

38 A. Albini and S. Monti, *Chem. Soc. Rev.*, 2003, **32**, 238-250.

39 Y. Ji, L. Zhou, Y. Zhang, C. Ferronato, M. Brigante, G. Mailhot, X. Yang and J.-M. Chovelon, *Water Res.*, 2013, **47**, 5865-5875.

40 H. Lignell, S. A. Epstein, M. R. Marvin, D. Shemesh, B. Gerber and S. Nizkorodov, *J.*

Phys. Chem. A, 2013, **117**, 12930-12945.

41 J. Eriksson, S. Rahm, N. Green, Å. Bergman and E. Jakobsson, *Chemosphere*, 2004, **54**, 117-126.

42 M. Czaplicka, *J. Hazard. Mater.*, 2006, **134**, 45-59.

43 S. Rayne, K. Forest and K. J. Friesen, *Environ. Int.*, 2009, **35**, 425-437.

44 W. J. Cooper and R. G. Zika, *Science*, 1983, **220**, 711-712.

45 J. L. Bolton, M. A. Trush, T. M. Penning, G. Dryhurst and T. J. Monks, *Chem. Res. Toxicol.*, 2000, **13**, 135-160.

46 S. Zhao, A. Narang, X. Ding and G. Eadon, *Chem. Res. Toxicol.*, 2004, **17**, 502-511.